Non-linear Stability Analysis of Cells Having Different Types of Cathode Surface Geometry

Marc Dupuis[1] and Valdis Bojarevics[2]

[1] GéniSim Inc., 3111 Alger St., Jonquière, Québec, Canada G7S 2M9
marc.dupuis@genisim.com

[2] University of Greenwich, School of Computing and Mathematics,
30 Park Row, London, SE10 9LS, UK
V.Bojarevics@gre.ac.uk

Keywords: Modeling, MHD, cell stability, irregular cathode surface, current density

Abstract

Different operational parameters are known to influence cell stability like ACD, ledge toe position and metal level.

Irregular cathode surface design is also thought to influence cell stability but how significantly as compared to the above operational parameters?

In the present work, cell stability analyses are performed on 3 types of cathode surface geometries: cathode with a flat surface, cathode with longitudinal ridges and cathode with lateral ridges.

Introduction

Irregular cathode surface technology is still the subject of research in China where it is quite popular. Chinese research papers recently published at the TMS [1-3] are concluding that irregular cathode surface technology is increasing cell stability, yet they are not presenting any results of cell stability analysis.

If we analyze the impact of irregular cathode surface technology one element at the time in mathematical model results, it has been observed that:

1) The irregular cathode surface technology has some effect on the drag of the cathode surface on the metal flow which is could be beneficial to the cell stability [4];

2) The irregular cathode surface technology has significant impact on the metal pad horizontal current which is more probably harmful than beneficial to the cell stability [2-3,5-6];

3) The irregular cathode surface technology may or may not have a significant impact on the global steady-state metal flow pattern and bath-metal interface deformation. Results reported so far are not in agreement, [1] and [2] report a significant change while [3] and [7] report far less changes;

4) A cell stability analysis is required to make any prediction of the impact of irregular cathode surface technology on the cell stability. Only [5-7] have presented results of that kind of cell stability analysis, a full non-linear transient analysis and results indicate that irregular cathode surface technology has little impact on the cell stability if other factors like the changes of ledge toe thickness or metal pad height are removed.

In order to make the above interpretation more rigorous, a new more thorough cell stability study had been carried out. Results of that more global cell stability study are now presented.

Cell stability study on a standard flat cathode surface cell

Before comparing the stability of cells using different type of cathode surface geometry, the present study will first cover more standard factors that are known to influence cell stability like ACD, metal pad level, ledge toe position and busbar design.

500 kA cell with regular flat cathode surface base case

The cell design that will be used as comparison base is the same as the one used in some previous work [5,7,8]. It is a 500 kA cell using a asymmetric busbar network design inspired from Chinese busbar design [9]. Figure 1 shows the model geometry as constructed by the most recent MHD-Valdis code version (July 2014):
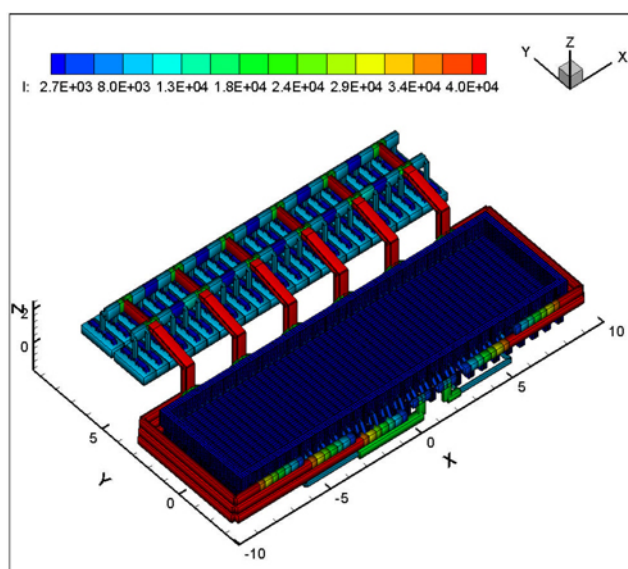
Figure 1: Geometry of the 500 kA base case model showing the current intensity solution in each conductor (in A)

After a few seconds of calculation, the above graphic, showing the busbar current, becomes available as well as the metal pad current density as shown in Figure 2.

The iso-contours are showing the current density at the surface of the cathode while the vectors are illustrating the horizontal components of the current density at the middle of the metal pad.

Then after a few minutes of calculation that takes into consideration the non-linear magnetization of the potshell and the

position of the return line (that have been moved as compared to previous publications), the magnetic field solution becomes available. Figure 3 is showing Bz, the vertical component of the magnetic field at the middle of the metal pad.
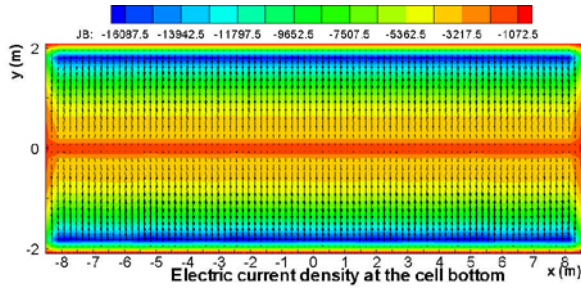

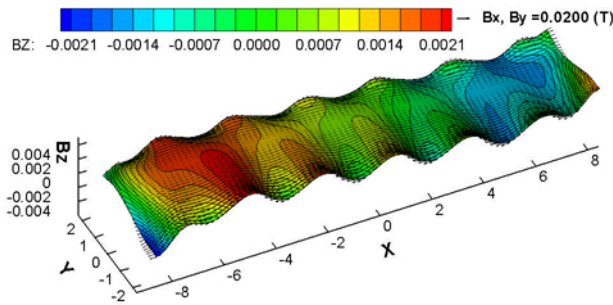**Figure 2: Current density solution on the top surface of the cathode (in A/m^2)**

Figure 3: Vertical component of the magnetic field solution in the middle of the metal pad (in T)

Then follow after about 15 to 20 minutes of calculation, the steady state solution of the bath-metal interface and metal flow pattern as presented in Figures 4 and 5 respectively:
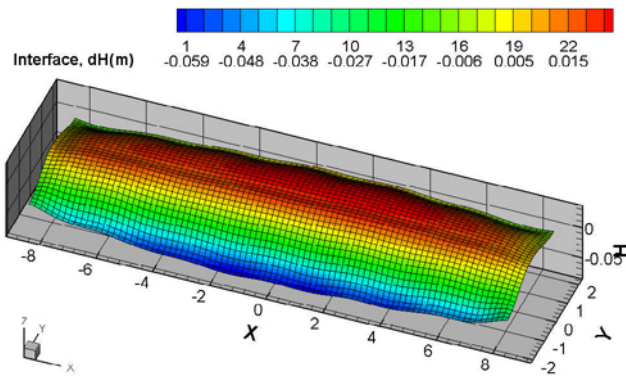

Figure 4: Steady-state bath-metal interface deformation (in cm) (0 is the position of the flat interface)

Since the CFD model is using the k-ω turbulence model k the turbulent kinetic energy is also available as scalar field as well as the two horizontal velocity components. In Figure 5, the magnitude of the vectors is used as scalar field. MHD-Valdis 2D shallow layer CFD model takes into consideration the topology of both the cathode surface and the bath-metal interface.
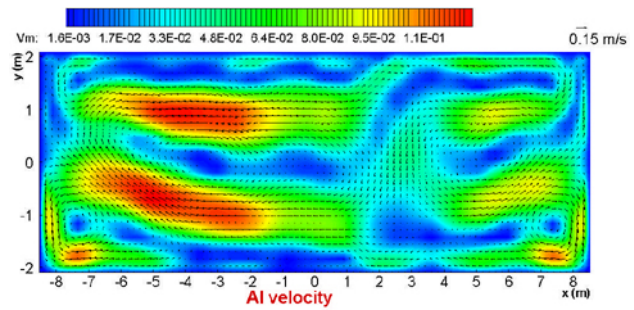

Figure 5: Steady-state flow pattern in metal pad (in m/s)

The fully non-linear transient analysis starts from that steady-state solution. Contrary to previous code version, the interface will not move at all if no initial perturbation is defined by the user. In previous versions [5-7], the transient analysis was starting with a high frequency wave that was being damped for about 150 seconds of transient evolution before a more unstable lower frequency wave could developed (Figure 18 of [5] is a good example of that) so a long transient analysis of about 1000 seconds was required to be able to evaluate the cell stability.

With the current code version, the user can define a perturbation that immediately triggers a 3,1 mode rotating wave that is typically the less stable wave mode. Figure 6 presents the results of a 1100 seconds fully non-linear transient analysis using the recommended 0.25 second time step. This type of transient analysis requires about 3 days of CPU on an Intel T9300 processor running on Windows x64.
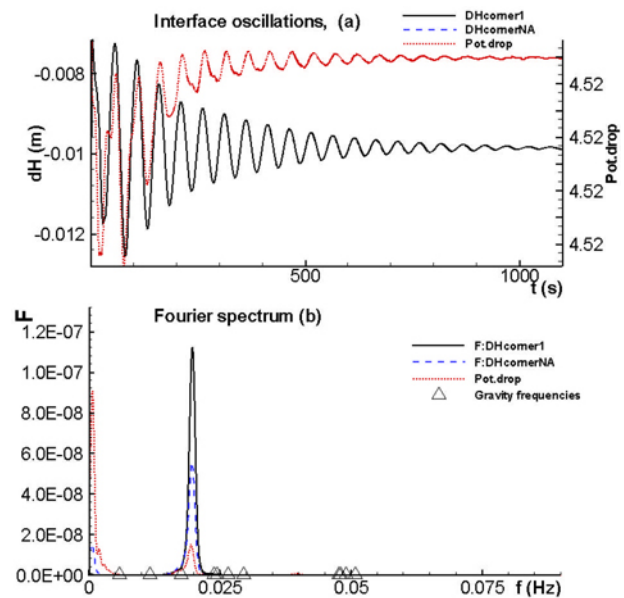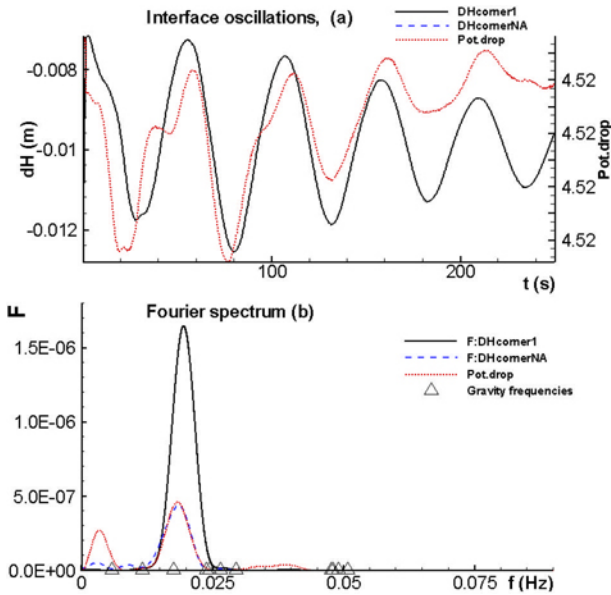

Figure 6: Evolution of one point on the interface position (in m) on the top and results of the spectral analysis of the wave evolution on the bottom

The evolution of the interface oscillations and the Fourier spectrum presented in Figure 6 clearly indicated that a single 3,1 rotating mode wave having a frequency just above the 3,0 gravity wave mode is being exponentially damped after an initial period of less than 100 seconds of more complex evolution.

Since the aim of the present study was to analyze a lot of different cases, a 250 seconds transient analysis duration was selected as standard duration to perform all those analyses. Figure 7 presents the results of that much shorter transient analysis.


Figure 7: Evolution of one point on the interface position (in m) on the top and results of the spectral analysis of the wave evolution on the bottom of a shorter 250 seconds analysis

The interpretation of the results is the same, a single 3,1 rotating wave is exponentially decaying after its initial formation phase for an unambiguous prediction of stable cell design for this base case model setup in less that 24 hours of CPU time.
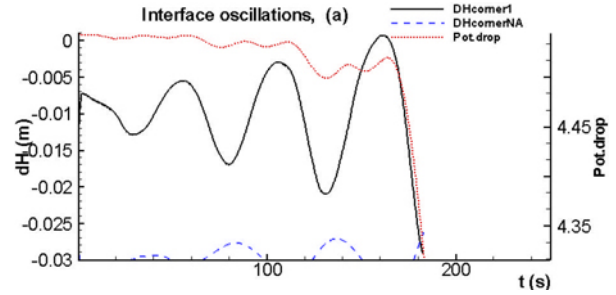
Base case minus 5 mm ACD

As can be seen in Figure 8, reducing the ACD from 4.5 cm to 4.0 cm is enough to flip the cell stability prediction from stable to unstable.
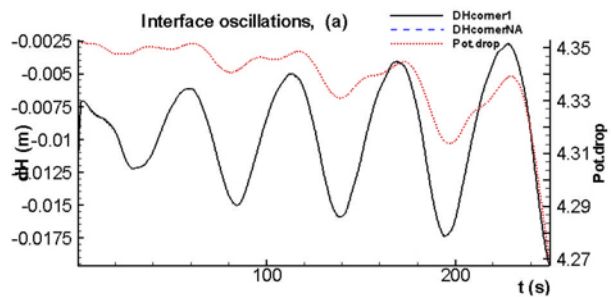
Figure 8: Stability analysis for base case minus 5 mm ACD

Base case minus 5 cm metal pad level

As illustrated in Figure 9, reducing the metal pad level from 25 cm to 20 cm is also enough to flip the cell stability prediction from stable to unstable. Since the wave is growing faster than in the previous case, the cell short circuits in about 180 seconds.

Figure 9: Stability analysis for base case minus 5 cm metal pad level
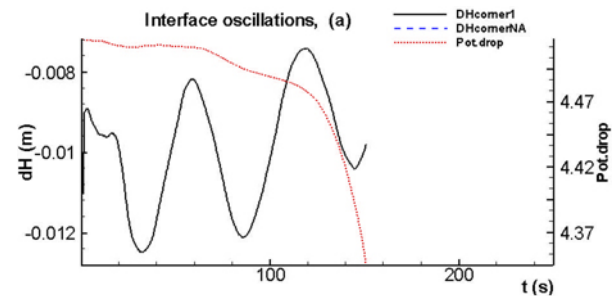
Base case plus 15 cm ledge toe thickness

Adding 15 cm of ledge toe thickness strongly affects a lot the metal pad current density as can be seen in Figure 10 below:
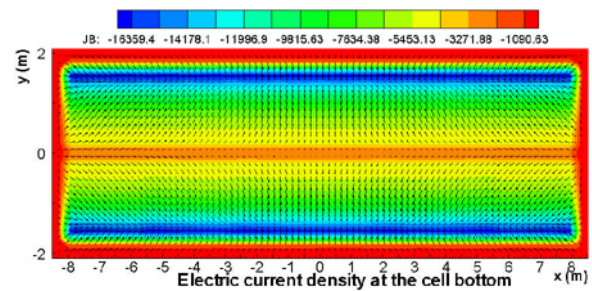
**Figure 10: Current density solution for base case plus 15 cm ledge toe thickness**

In turn, this increase of metal pad horizontal current significantly decreases the cell stability. As shown in Figure 11 below, the wave is growing even faster than in the previous case, the cell short circuits in about 150 seconds.

Figure 11: Stability analysis for base case plus 15 cm ledge toe thickness

Improved magnetic field case

The previous four cases are demonstrating that the selected base case busbar design is stable but is quite close to the stability limit which is a good thing to highlight the impact of destabilizing actions on the cell. The next case, on the contrary, highlights the stabilizing effect of improving the magnetic field by improving the busbar network design in order to reduce the Bz gradient intensity.
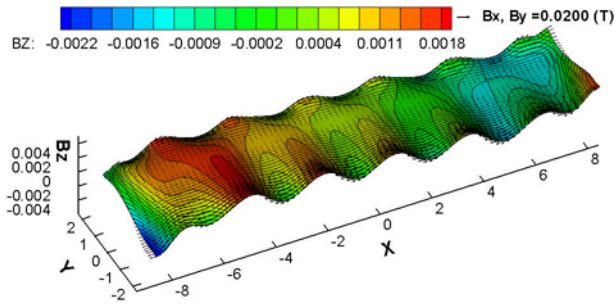
Figure 12: Vertical component of the magnetic field solution from the improved busbar design case

In order to improve the magnetic field, the return line was moved away 5 m from 60 to 65 m in addition to moving a few busbars around the cell. The Bz field looks very similar in Figure 12 as compared to Figure 3 but the quarter averaged values available in the printout are now more symmetric. For the base case, the results were:

```
Quarter averages of BSZ in T


            ^ Y
            |
  0.00127|  -0.00056
----------|----------> X
  0.00105|  -0.00033
            |
```

while for the improved magnetic field case, the results were:

```
Quarter averages of BSZ in T


            ^ Y
            |
  0.00098|  -0.00048
----------|----------> X
  0.00073|  -0.00020
            |
```

This is a clear improvement of the magnetic field as the gradient of the Bz in the longitudinal direction of the cell (X direction), that is the generator of the 3,1 mode rotating wave [10], has been significantly decreased. As a result, the stability analysis reports a more stable cell as the wave damping rate has significantly increased as shown in Figure 13:
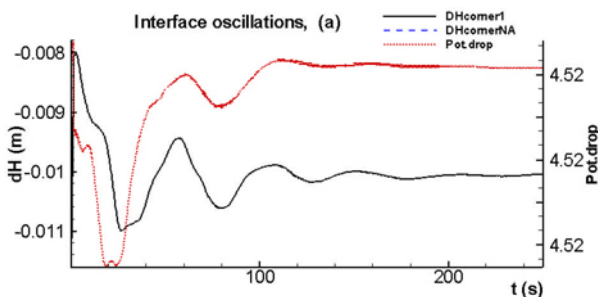
**Figure 13: Stability analysis for the improved magnetic field case**

Lateral ridges case

The lateral ridges case was built as follow. There are 48 collector bars per side in that cell and normally 24 blocks using a double bars per block arrangement. In order to generate well resolved lateral rides considering the 80x30 mesh resolution of the CFD model, the 24 blocks double bars per block arrangement was replaced by a 48 blocks single bar per block arrangement with a unit of three repetitive patterns, where the first and third blocks remained the same height, but the height of the second block has been increased by 10 cm. This scheme generates 16 lateral ridges in the cell. Figure 14 is showing a zoom in view of the cathode surface geometry.
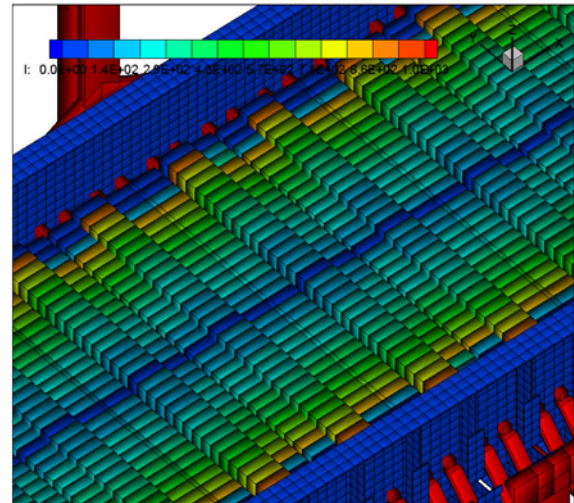

Figure 14: Geometry of the lateral ridges case showing the current intensity solution in each conductor (in A)

MHD-Valdis offers the option to define the position of the ledge toe all around the perimeter of the cell. That option was used here to define the base case thickness on top of ridges and a plus 15 cm thickness between ridges in order to represent the ledge toe thickness presented in Figure 5 of [11]. The resulting metal pad current density is presented in Figure 15:
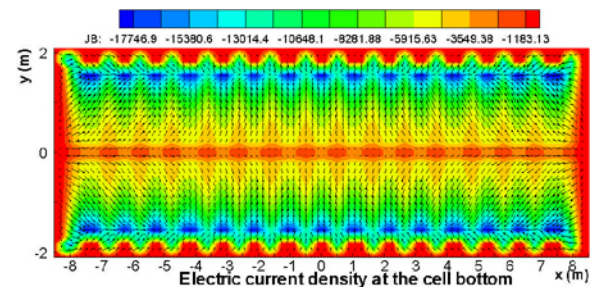

Figure 15: Current density solution on the top surface of the cathode (in A/m^2) for the lateral ridges case

The resolution of the ridges geometry by the 80x30 CFD model mesh is shown in Figure 16. Clearly a much finer mesh would be required to represent adequately a bigger number of narrower ridges (see per example Figure 6 of [3]) which would in turn increases the time required to carry up a cell stability analysis.
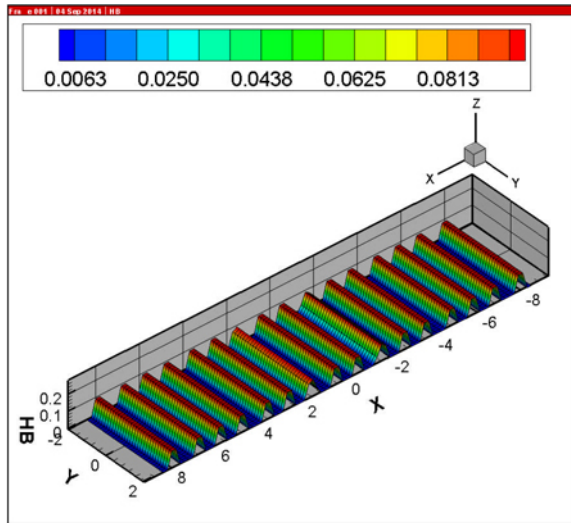
Figure 16: Spatial resolution of the 16 ridges geometry in the 80x30 CFD model mesh

The impact of the ridges is also clearly visible in the steady-state solution presented in Figures 17 and 18. Note that, in order to keep unchanged the metal volume, the metal pad level has been increased to 28.33 cm from the 25 cm base case.
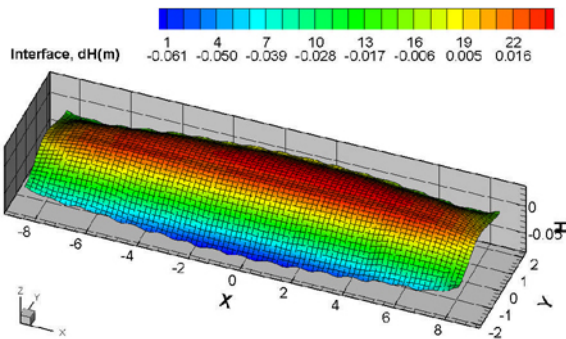

Figure 17: Steady-state bath-metal interface deformation (in cm) for the lateral ridges case
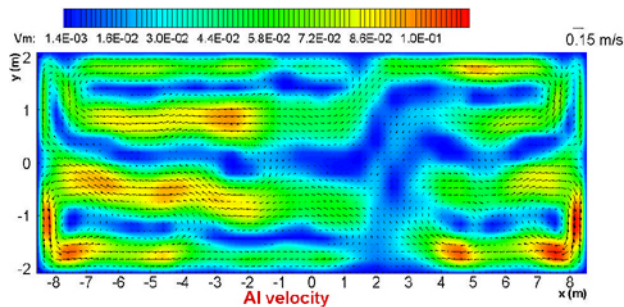
Figure 18: Steady-state flow pattern in metal pad (in m/s) for the lateral ridges case

To be fair the lateral ridges case stability should not be compared to the base case but to the base case plus 15 ledge toe thickness, and there is no substitute for performing the cell stability analysis to know if this lateral ridges case will turn out to be more or less stable than the base case plus 15 ledge toe thickness. Results of the transient cell stability analysis are presented in Figure 19.
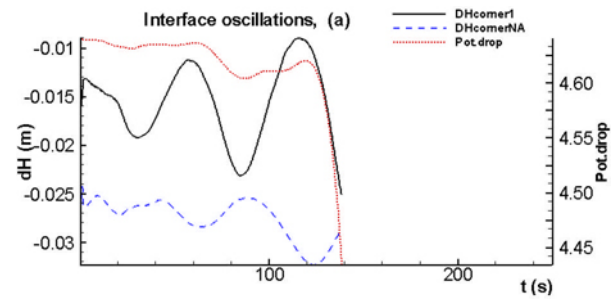

Figure 19: Stability analysis for the lateral ridges case

The cell is still predicted to be unstable with a wave growth rate very similar to the one of the base case plus 15 ledge toe thickness as the cell short circuit in about 140 seconds. Again in this study, the prediction of MHD-Valdis is that the presence of lateral ridges should not affect much the cell stability.

Longitudinal ridges case

The longitudinal rides case was built as follow. In [5] and [6], the impact of a cell having 8 longitudinal ridges on the metal pad current density was analyzed using a detailed finite element thermo-electric model. Unfortunately, 30 mesh divisions in the lateral direction is not enough to well discretize 8 longitudinal ridges, so this case will study the impact of adding 6 longitudinal ridges on the cell stability instead. Figure 20 shows the spatial resolution of those 6 ridges, while Figure 21 shows the resulting metal pad current density. Note that this time, the base case ledge toe thickness was kept.

The impact of the ridges is also clearly visible in the steady-state solution presented in Figures 22 and 23. Note that in order to keep unchanged the metal volume, the metal pad level has been increased to 28.33 cm again this time.
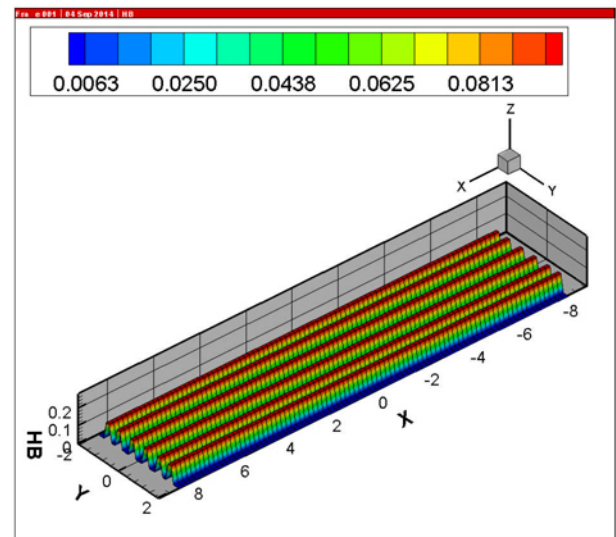
Figure 20: Spatial resolution of the 6 ridges geometry in the 80x30 CFD model mesh
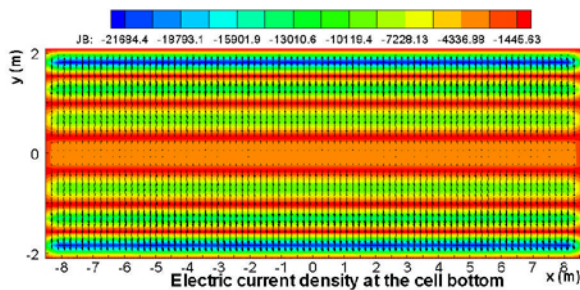
Figure 21: Current density solution on the top surface of the cathode (in A/m^2) for the longitudinal ridges case
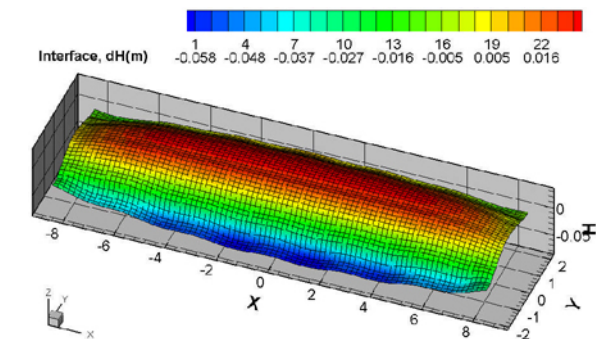

Figure 22: Steady-state bath-metal interface deformation (in cm) for the longitudinal ridges case
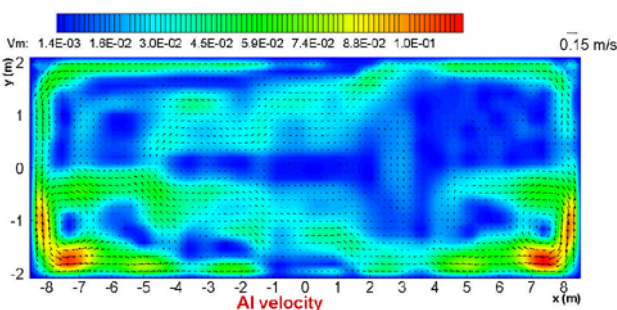

Figure 23: Steady-state flow pattern in metal pad (in m/s) for the longitudinal ridges case
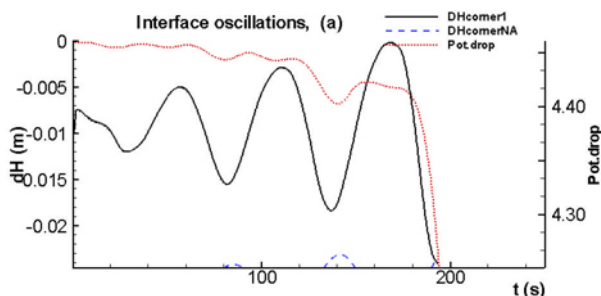

Figure 24: Stability analysis for the longitudinal ridges case

According to the stability analysis results, the addition of longitudinal ridges destabilize the cell.

Conclusions

A thorough cell stability study has been carried out for a standard flat cathode surface cell. As expected, reducing the ACD, reducing the metal pad level and increasing the ledge toe thickness has a destabilizing effect on the cell. As expected as well, reducing the longitudinal gradient of the Bz has a stabilizing effect on the cell.

As reported in previous study [5,7], the prediction of MHD-Valdis is that the presence of lateral ridges should not affect much the cell stability.

When the impact of the longitudinal ridges on the metal pad current density reported in [5,6] is taken into consideration, the prediction of MHD-Valdis is that their presence has a destabilizing effect on the cell.

References

[1] Qiang Wang, Jianping Peng, Baokuan Li and Naixiang Feng, "Effect of innovative cathode on bath/metal interface fluctuation in aluminum electrolytic cell" TMS Light Metals 2014, 491-494.

[2] Wang Qiang, Li Baokuan, Wang Fang, Feng Naixiang, "Magnetohydrodynamic model coupling multiphase flow in aluminum reduction cell with innovative cathode protrusion", Light Metals 2013, 615-519.

[3] Baokuan Li, Fang Wang, Xiaobo Zhang, Fengsheng Qi and Naixiang Feng, "Modeling of interface of electrolyte/aluminum reduction cell with novel cathode structure", TMS Light Metals 2012, 865-868.

[4] Valdis Bojarevics, "MHD of Aluminium Cells with the Effect of Channels and Cathode Perturbation Elements," TMS Light Metals 2013, 609-614.

[5] Marc Dupuis and Valdis Bojarevics, "Influence of the cathode surface geometry on the metal pad current density", TMS Light Metals 2014, 479-484.

[6] Valdis Bojarevics and Sharnjit Sira, "MHD stability for irregular and disturbed aluminium reduction cells", TMS Light Metals 2014, 685-690.

[7] Marc Dupuis and Valdis Bojarevics, "Newest MHD-Valdis cell stability studies", ALUMINIUM, 90 (2014) 1-2, 42-44.

[8] Marc Dupuis and Valdis Bojarevics, "Retrofit of a 500 kA cell design into a 600 kA cell design", 87 (2011) 1-2, 52-55.

[9] Hongliang Zhang, Chenn Q. Zhou, Bing Wu and Jie Li, "A Virtual Aluminum Reduction Cell", JOM, Vol. 65, No. 11, 2013, 1452-1458.

[10] Nobuo Urata, "Wave mode coupling and instability in the internal wave in aluminum reduction cells", TMS Light Metals 2005, 455-460.

[11] J. Zhou et al., "Depth Analysis and Potential Exploitation of Energy-Saving and Consumption-Reduction of Aluminum Reduction Pot," TMS Light Metals, 2012, 601-606.